

A Novel Capsule Neural Network Based Model for Drowsiness Detection Using Electroencephalography Signals

Luis Guarda^a, Juan Tapia^b, Enrique Lopez Droguett^a, Marcelo Ramos^c.

^a*Mechanical Engineering Department, University of Chile, Santiago, Chile*

^b*da/sec-Biometrics and Internet Security Research Group, Hochschule Darmstadt, Germany.*

^c*Analysis, Evaluation and Risk Management Laboratory – LabRisk, Naval Architecture, Sao Paulo, Brazil.*

This is a pre-print version. Full version will be available in Expert Systems With Application

Abstract

The early detection of drowsiness has become vital to ensure the correct and safe development of several industries' tasks. Due to the transient mental state of a human subject between alertness and drowsiness, automated drowsiness detection is a complex problem to tackle. The electroencephalography signals allow us to record variations in an individual's brain's electrical potential, where each of them gives specific information about a subject's mental state. However, due to this type of signal's nature, its acquisition, in general, is complex, so it is hard to have a large volume of data to apply techniques of Deep Learning for processing and classification optimally. Nevertheless, Capsule Neural Networks are a brand-new Deep Learning algorithm proposed for work with reduced amounts of data. It is a robust algorithm to handle the data's hierarchical relationships, which is an essential characteristic for work with biomedical signals. Therefore, this paper presents a Deep Learning-based method for drowsiness detection with CapsNet by using a concatenation of spectrogram images of the electroencephalography signals channels. The proposed CapsNet model is compared with a Convolutional Neural Network, which is outperformed by the proposed model, which obtains an average accuracy of 86,44 % and 87,57% of sensitivity against an average accuracy of 75,86% and 79,47% sensitivity for the CNN, showing that CapsNet is more

*Corresponding author. E-mail address: juan.tapia-farias@h-da.de

Email addresses: juan.tapia-farias@h-da.de (Juan Tapia), elopezdroguett@ing.uchile.cl (Enrique Lopez Droguett), mrmartin@usp.br (Marcelo Ramos)

suitable for this kind of datasets and tasks.

Keywords: Deep Learning, Drowsiness, Electroencephalography, Capsule Neural Network, Convolutional Neural Network.

1. Introduction

In the last decades there has been a sustained increase in the level of automation of work environments, which has meant that it becomes increasingly common the execution of monotonous tasks that require a high level of attention (Hockey et al., 2003). When these tasks are intended to ensure the correct and safe operation in work environments such as control rooms, it is essential to ensure that operators maintain an adequate level of alertness. In this context, the early detection of drowsiness in operators has become of vital importance to guarantee the reliability of the operation.

Drowsiness is defined as a middle state between slumber and alertness, where the subject has an overwhelming desire to sleep. These symptoms are accompanied by an increase in the reaction times of the subject and, consequently, a reduction in his or her surveillance capacity. As an example, in the incidents of Three Mile Island and Chernobyl, drowsiness was documented as a contributing factor. In this context, drowsiness is usually used interchangeably with the term mental fatigue, even though mental fatigue is considered a broader concept (Trejo et al., 2015; Ramzan et al., 2019).

Through the use of electroencephalography signals (captured from several electrodes located on the scalp), it is possible to record the bioelectrical activity generated by the cortical neurons of the brain and their variation in time, which provide information about the mental state of the subject. Particularly, the measurement of the frontals and parietals channels can be used to analyze the level of drowsiness of a subject due the variations on the amplitude in the frequencies range of theta and alpha waves that can be tracked in these channels (Trejo et al., 2015; Barua et al., 2019). On the other hand, studies have found that there exist a relationship between the amplitude variations of alpha and theta waves in a drowsy subject with the Karolinska sleepiness scale (Kaida et al., 2006), which measures the level of self-perceived sleepiness of an individual into nine scores (Akerstedt & Gillberg, 1990). However, the detection of drowsi-

ness has not been limited to the use of electroencephalography signals. Several authors have used parallel and / or complementary inputs such as the use of electrocardiography signals (Chui et al., 2015), and eye tracking devices (Yeo et al., 2009), through the use of machine learning algorithms. The main limitation of this type of methods is that they are based on the extraction and selection of features in a handcrafted way, which are subject to the uncertainty and bias of the experts in charge of the manual feature engineering. Although the methods of eye tracking have achieved good results, the use of video devices makes these techniques too invasive for the operator's privacy.

In this context, Deep Learning techniques are presented as a valid alternative to replace the methods of extraction and selection of handcrafted features, thanks to their ability to learn how to identify specific features of their environment autonomously (LeCun et al., 2015), thus avoiding the need to have experts in each area that direct the learning.

Using Deep Learning algorithms, several authors have used EEG signals to achieve the detection of different classification tasks. As an example, (Zheng et al., 2019) use a Deep Neural Network in combination with a six-electrode EEG to classify human emotions, and in (Spampinato et al., 2017) authors use Recurrent Neural Networks (RNN) and a Convolutional Neural Network (CNN) to learn visual stimuli-evoked data from EEG signals and classify and then reconstruct object classes from the ImageNet dataset (Deng et al., 2009).

Nonetheless, the use of Deep Learning algorithm has not been limited to the use of raw signals as input. Spectrograms of the corresponding signals as input data have attracted many authors (Yuan L., 2018; Lees et al., 2019; Lee et al., 2009). In this context, Verstraete et al. developed a CNN based model (Verstraete et al., 2017) able to carry out the fault diagnosis of ball bearings through the use of spectrograms from vibration signals of the rolling elements analyzed, achieving better results in the classification task than conventional shallow methods of manual feature extraction and selection.

However, Convolutional Neural Networks have shown to have two main problems. First, they require large volumes of data for training, which is an inherent problem when working with bioelectric signals. Secondly, due to the loss of information that occurs in the pooling layer of the CNN's, there is a positional invariance of the compo-

nents that the network uses to carry out the classification, which prevents it from being sensitive to changes of rotation or translation within the image (Sabour et al., 2017). One way to eliminate this problem is with excessive training for all of the possible angles, but it usually takes a greater dataset and a lot more time and computational resources. This positional invariance represents a problem when it comes to dealing with transient 1-D signals such as electroencephalography signals.

In this context, Capsule Neural Networks (CapsNet) were recently introduced as a Deep Learning technique which seeks to solve CNNs problems through the replacement of the pooling layer by a routing-by-agreement algorithm and the replacement of the use of scalars within the network by capsules (vectors) (Sabour et al., 2017). These changes allow this type of network to work with a smaller amount of data and can establish equivalence relationships between the characteristics of the images.

The CapsNet architecture introduced in (Sabour et al., 2017) not only allowed us to solve the inherent problems of CNNs, but it also reached state-of-the-art results for the MNIST dataset (LeCun & Cortes, 2010). For this reason, CapsNet based models have seen a surge in the recent literature with applications in a variety of fields as a variety of areas such as the work of Xi et al (Xi et al., 2017; Hinton et al., 2018).

Moreover, in (Upadhyay & Schrater, 2018), the authors proposed a Generative Adversarial Networks (GANs) that employs a CapsNet as the discriminator. Rawlinson et al. (David Rawlinson, 2018) perform an unsupervised training of latent capsule layers using only the reconstruction loss as input, obtaining a better generalization than the supervised model for the affNIST and MNIST benchmarks datasets. CapsNets have been also applied to process biomedical data as, for example, in (LaLonde & Bagci, 2018) where the authors expand CapsNets to work with large images of lungs computed tomography scans, and Afshar et al. (Afshar et al., 2018) use CapsNets to tackle the brain tumor type classification task, outperforming the performance of CNN in the same problem.

Due the aforementioned limitations of CNNs to work with reduced volumes of data and for being incapable of handling changes in rotation or translation of the input data, we propose a Capsule Neural Network that is able to work with EEG signals in order to tackle the problem of drowsiness detection, thus using the advantages of CapsNet over

CNNs to achieve a higher capability of generalization and accuracy, and also avoiding the manual extraction of features which introduce a bias to the algorithm.

The proposed Capsule Neural Network model for drowsiness detection makes use of spectrograms from electroencephalogram signals as input. Moreover, the spectrograms were obtained from the frontal Fz and parietal Pz channels due to the relationship between these channels and the variations in amplitude of alpha and theta waves when a subject is under a drowsiness state (Trejo et al., 2015). Also, two spectrograms datasets are considered: the first one corresponds to spectrograms from EEG signals of the Fz channel, whereas the second dataset corresponds to the vertical concatenation of spectrograms obtained from both the Fz and Pz channels.

The proposed CapsNet model's performance in the drowsiness detection task is also compared to a deep Convolutional Neural Network model as well as other shallow machine learning models such as Neural Networks (Schmidhuber, 2015), Support Vector Machines (Cortes & Vapnik, 1995) and Random Forests (Breiman, 2001).

The paper is organized as follows. Section 2 provides an overview about the background of drowsiness, electroencephalography, CNNs and CapsNets. Section 3 presents the datasets used to carry out the detection of drowsiness and the pre-processing methodology applied to the EEG signals as well as comparisons of the proposed CapsNet model with CNN, SVM, Random Forest and shallow neural network. Section 4 present the experiments. Section 5 the results and discussion, finally section 6 with the concluding remarks.

2. Background

2.1. Drowsiness

Drowsiness can be described as the set of psychological and physiological changes that a subject suffers while executing a task that requires a high level of attention for a great period of time. Drowsiness is manifested as a deterioration in the cognitive and psychomotor proficiency of the individual, which results in a reduced alertness, accompanied by a lack of energy (Marek et al., 1988). In this way, drowsiness can be

understood as the loss of a subject's basic abilities, such as reacting in a timely and appropriate manner to an unforeseen event (ASCH, 2007).

When an individual is in a state of drowsiness, the following symptoms may appear:

- Slow or clumsy movements.
- Decrease in the motor speed of reaction.
- Appearance of blurred or double vision.
- Difficulty remembering.
- Difficulty concentrating or staying alert.

From this perspective, an individual who works under the effects of drowsiness in an environment that requires a high level of attention can provoke an accident (ASCH, 2007).

2.2. *Electroencephalography*

Electroencephalography (EEG) is an electrophysiological monitoring method that allows the recording of the bioelectrical activity generated by the cortical neurons of the brain and their variation over time. This technique is carried out by placing small electrodes on the subject's scalp. The signals picked up by the electrodes are delivered to an electroencephalograph, which amplifies the brain wave potentials ¹

To guarantee the standardized reproducibility of the captured EEG signals, the international 10-20 electrode placement system (Homan, 1988), which is based on the relationship between the location of an electrode and the underlying area of the electrode cerebral cortex. Figure 1 shows the traditional disposition of the electrodes for the international system 10-20.

The EEG signals can be divided into four segments depending on their frequency band. Each of these bands refers to different states of consciousness such as sleep, intense mental activity, and drowsiness. These four frequency bands are the following:

¹https://www.trans-cranial.com/docs/10_20_pos_man_v1_0_pdf.pdf

- Delta (0.5-4Hz): its appearance occurs mainly during deep sleep.
- Theta (4-8Hz): this type of wave is characterized by a state of drowsiness of the individual with reduced consciousness.
- Alpha (8-13Hz): it represents a state of low brain activity and relaxation both physical and mental, but aware of the environment.
- Beta (13-20Hz): waves of this type are emitted when a subject is in a conscious or alert state. Beta waves denote intense mental activity.
- Gamma (> 30Hz): its appearance is associated with large-scale brain network activity such as attention and working memory(Nie, 2017).

In the context of drowsiness detection, the frontal and parietal channels provide information about the level of drowsiness of an individual, which is represented in variations of the alpha and theta waves (Trejo et al., 2015).

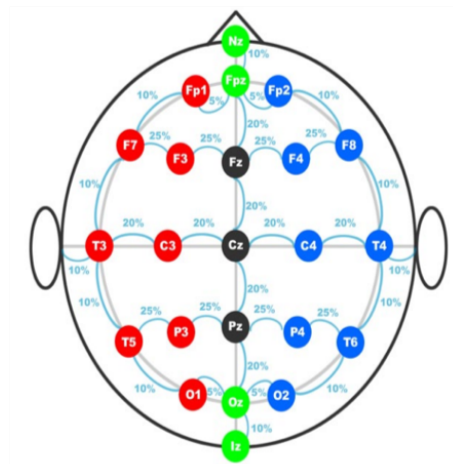


Figure 1: International electrode placement system 10-20 (Homan, 1988).

2.3. Karolinska Sleepiness Scale

In order to avoid detection of fatigue events where the subject perceives himself as alert (False positive), it is possible to label the EEG data for sleepiness using the

Karolinska Sleepiness Scale (KSS). This scale measures the level of self-perceived sleepiness for the individual in the last 10 minutes, and a significant relationship has been found between the variation of alpha and theta waves and the KSS (Kaida et al., 2006; Akerstedt & Gillberg, 1990). Table 1 shows the description of each level of the scale, which has a range from 1 to 9.

Table 1: Karolinska Sleepiness Scale [4].

Scale	Psychophysical state
1.	Extremely alert
2.	Very alert
3.	Alert
4.	Rather alert
5.	Neither alert nor sleepy
6.	Some signs of sleepiness
7.	Sleepy, but no difficult remaining awake
8.	Sleepy, some effort to keep alert
9.	Extremely sleepy, fighting sleep

2.4. Convolutional Neural Network

Convolutional Neural Networks (CNN) are a Deep Learning algorithm developed to tackle matrix (structures) data such as images. CNNs are composed of three types of layers: convolution layer, pooling layer and classification layer (Goodfellow et al., 2016). Due to this arrangement, CNNs can reduce dimensionality and learn specific non-linear representations. The specific function of each layer can be summarized as follows (see Figure 2 and Figure 3):

- **Convolutional layer:** in this first layer, a convolution between the input image and multiple local filters is made, generating different invariant local features for each kernel (filter) applied. This process allows certain characteristics of the input data to become more dominant in the output. In Equation (1), a convolution

between a two-dimensional input (I) and a two-dimensional kernel (K) is shown:

$$S(i, j) = (I * K)(i, j) = \sum_m \sum_n I(i + m, j + n)K(m, n) \quad (1)$$

- Pooling layer:** usually the pooling layers are located after a convolutional layer. The function of this type of layer is to extract the most significant features of the output of the previous layer. This features extraction is done performing a sampling reduction, which implies a loss of information(Sabour et al., 2017), but it also leads to a lower calculation overload, and introduces translational invariance to the model, which allows the model to be less susceptible to small changes in the input, reducing the possibility of overfitting (Boureau et al., 2010). The sampling reduction that occurs in the pooling layers implies that the network is not able to reconstruct the input after a pooling layer because the characteristics that were not selected are dropped and cannot be used again. In the same way, after a pooling layer, the network forgets wherein the data and how many times (inside the pooling filter size) each feature appears. On the other hand, the max-pooling function is one of the possible choices to use in this layer. This operation finds the maximum value between sample windows, saving only these values for the next layer. In Figure 2, the operation performed by the max-pooling can be observed graphically.

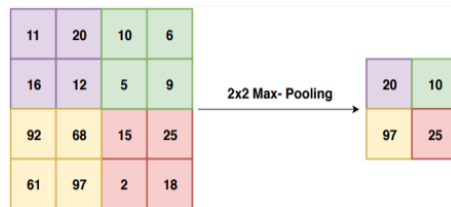


Figure 2: Example of 2x2 max pooling.

- Classification layer** subsequently the convolution and pooling layers, one or more fully connected layers of neurons can be used, in which each pixel of the last output layer is considered as an input to an individual neuron. Using this input, the fully connected layer performs the desired classification.

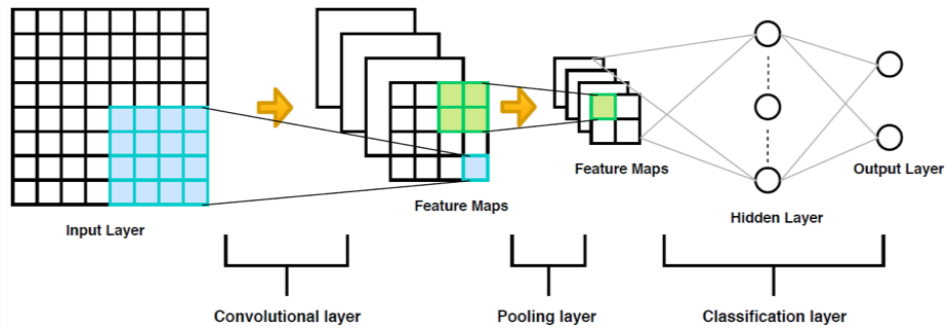


Figure 3: Generic CNN Architecture.

2.5. Capsule Neural Network: An Overview

Through the pooling operation, CNNs are able to perform dimensionality reduction and to add a certain degree of translational invariance to the model. This results in a reduction of the required computational cost in classification (i.e., diagnostics) tasks, whereas the translational invariance allows the model to identify small changes in the inputs, improving its generalization capability (Boureau et al., 2010).

However, the above-mentioned aspects of CNNs have some inherent problems. Indeed, the translational invariance only makes the network less sensitive to small changes of translation, but it is not able to deal with rotations or different angles of the same input. Also, due to the loss of information that takes place in the dimensionality reduction operation, the network cannot keep the spatial and hierarchical relationships among the extracted features.

In order to tackle these inherent limitations of CNNs, Sabour et al (Sabour et al., 2017) introduced a novel algorithm for image recognition known as Capsule Neural Networks, which incorporates the concept of equivariance to the network, allowing the model to keep the spatial and hierarchical relationships among the extracted features. The generic architecture of CapsNet is composed by the following layers: input layer, convolutional layer, primary capsules, secondary capsules and finally the output as shown in Figure 4.

In this model, capsules are groups of neurons represented as vectors, where each

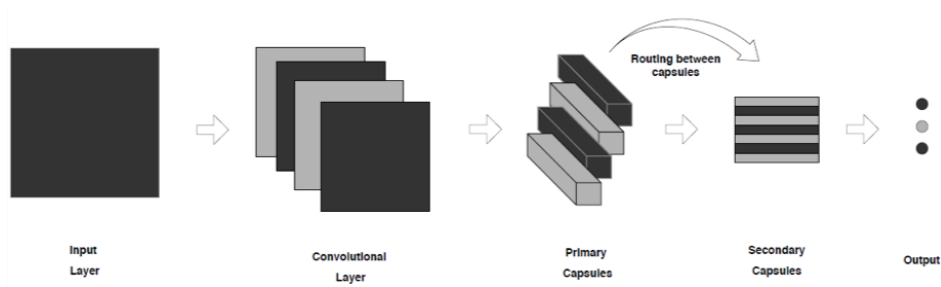


Figure 4: Generic Capsnet architecture.

neuron denotes a feature from an object and the length of the vector corresponds to the capsule's activation probability. To ensure that the vector length is between 0 and 1, a squashing function is applied as follows:

here v_j is the “squashed” value of the capsule's output s_j .

$$v_j = \frac{s_j^2}{(1 + s_j^2)} \times \frac{s_j}{s_j^2} \quad (2)$$

To get the first layers of capsules, the algorithm performs a convolution operation, with the extracted features maps being rearranged into vectors (with a previously given dimension) and are resized using Equation (2).

Then, in order to select which features are more predominant for the current prediction and thus avoiding the pooling process, Capsule Neural Networks use an iterative process called dynamic routing, which takes the predictions from primary capsules and computes the actual output according to an agreement metric between predictions.

The predictions of the actual output for each capsule are calculated using Equation (3):

$$\hat{u}_{(ji)} = w_{ij}u_i \quad (3)$$

where u_i is the output of capsule i , $\hat{u}_{(ji)}$ is the prediction of the j^{th} higher capsule given u_i and W_{ij} is the weighting matrix between capsule i and capsule j . The output of the j^{th} higher capsule s_j corresponds to a weighted sum over all $\hat{u}_{(ji)}$, which is

obtained using Equation (4) as:

$$s_j = \sum_i c_{ij} \hat{u}_{(ji)} \quad (4)$$

where c_{ij} are called coupling coefficients, and are calculated by Equation (5):

$$c_{ij} = \frac{\exp(b_{ij})}{\sum_k \exp(b_{ik})} \quad (5)$$

On the other hand, the coupling coefficients are calculated in an iteratively way by the dynamic routing process using Equation (6):

$$b_{ij} \leftarrow b_{ij} + \hat{u}_{(ji)} * v_j \quad (6)$$

where $\hat{u}_{(ji)} * v_j$ indicates the level of agreement between the actual output of the capsule and the prediction done by the corresponding capsule in the first layer (Sabour et al., 2017).

The number of iterations is previously defined, according to the classification task that is desired. Finally, the classification is made according to the prediction made by the capsules in the last iteration.

3. The Dataset

In this study, only the EEG signals and the KSS scores of the subjects were used. From the five EEG channels available for each subject, only the signals recorded by the frontal (Fz) and parietal (Pz) electrodes were used. This choice is based on the fact that alpha and theta waves show an increase of amplitude that can be measured in mentioned channels in case of the subjects is in the drowsy (Trejo et al., 2015).

In order to generate the labels of the EEG signals, the description of the KSS indexes was used. In this way, the data of the subjects that reported a KSS index (see Table 1) less than or equal to 4 were characterized as alert (no drowsiness), and the subjects who reported a KSS index greater than or equal to 7 were characterized as drowsy (Akerstedt & Gillberg, 1990). This labeling rule was applied only for the data

from PVT 1 and PVT 3 (see Figure 6), excluding the data from PVT 2 due to the average values of the KSS index of the PVT 2 (5, 6 + -1, 7), which do not correspond to any of the classes previously defined. On the other hand, it should be noted that none of the KSS indices of the PVT 3 corresponds to the alert state and none of the KSS indices of PVT 1 corresponds to the drowsy state. Thus, all the signals labeled as alert correspond to the PVT 1 and all the signals labeled as drowsy were obtained from the PVT 3. Once this is done, the data from 10 subjects from PVT 1 and the data from 10 subjects from PVT 3 satisfy the mentioned labeling rule. After the labeling process and with the aim of increasing the data size, the EEG signals (which originally had a duration of 10 minutes) from both channels Fz and Pz were segmented into files of thirteen seconds durations. This time interval corresponds to the minimal duration that an EEG signal must have to enclose all the subject mental alertness (Trejo et al., 2015). After this, the amount of data from each channel was 920 files with 460 for each class.

Then, a spectrogram was obtained for each file of thirteen seconds. The spectrograms were generated using 512 points as window size, an overlap of 50% and plotting only the frequencies from 0 to 20 Hz, given that one is interested only in the variations of alpha and theta waves (Trejo et al., 2015). The spectrograms were converted into grayscale, resulting in a size of $32 \times 32 \times 1$ pixels and the color bar and axes were removed.

Based on the abovementioned procedure, two sets of spectrograms were obtained, which are described below:

1. Spectrograms from channel Fz / 13 seconds duration: set of spectrograms from channel Fz with size of 32×32 pixels, a duration of thirteen seconds and a frequency range from 0 to 20 Hz.
2. Spectrograms from channels Fz-Pz / 13 seconds duration: set of spectrograms from both channels Fz and Pz concatenated vertically, resulting in 64×32 pixels, with a duration of thirteen seconds and a frequency range from 0 to 20 Hz.

Figure 5 show a spectrogram using a 512 windows size. A spectrogram was obtained for each file of thirteen seconds using the raw signal. The spectrograms were generated using 512 points as window size, an overlap of 50%, 512 discrete Fourier

transform points (NFFT) and plotting only the frequencies from 0 to 20 Hz, given that we are interested only in the variations of alpha and theta waves. The spectrograms were converted into grayscale, resulting in a size of $32 \times 32 \times 1$ pixels and the color bar and axes were removed.

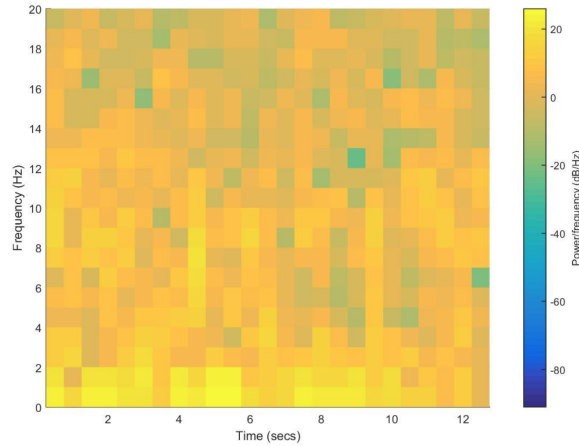


Figure 5: Example of EEG spectrogram obtained using a windows size of 512 points, an overlap of 50% and 512 discrete Fourier transforms points (NFFT).

4. Data-Augmentation

In the absence of an adequate volume of training data, it is possible to increase the proper size of existing data through data augmentation, which has contributed to significantly improving the convolutional neural network’s performance in the domain of image classification. In the case of ECG signal, data-augmentation (DA) can be applied to signal or spectrograms (Park et al., 2019; Pan et al., 2020). In this paper, a DA was applied directly to the spectrogram images to modify and improve the input images. Spectrogram masking blocks of consecutive frequency channels and masking blocks of utterances were modified. These augmentations have been chosen to help the network be robust against deformations in the time direction, partial loss of frequency information, and partial loss of small ECG segments of the input.

In this paper, it has been applied the data-augmentation based on the imaugaug library (Jung, 2018) to perform the various augmentation operations on images. Their

respective values used are Zoom range: 0.15, Width shift: 0.15, Fill mode: nearest, Brightness range: [0.5,1.5], Rotation angle: 10, Height shift: 0.10 and CoarseDropout: True. An important function is the “CoarseDropout” with a probability from 0.2 to 0.5. Drop 2% of all pixels by converting them to black pixels but do that on a lower-resolution version of the image with 50% of the original size, leading to 2×2 squares being dropped.

It must be mentioned that the augmented train dataset was used only to train the proposed CapsNet model, as it is the main focus of this work, in order to evaluate the performance of the model when it is trained with a bigger and more diverse dataset.

5. Experiments

To avoid obtaining biased results, all the results presented in this section were obtained using five-fold (holdout) cross-validation using 80% of the data for training and 20% for the test. Moreover, all the results presented in this section were obtained using a CPU Core i7-6700K 4.2 GHz with 32 GB ram and GPU Tesla K20, with Ubuntu 16.04, CUDA 9.0 and TensorFlow r1.8. All the metrics presented in this chapter were obtained using the formulas presented in (Sokolova & Lapalme, 2009).

5.1. Experiment 1.- The Proposed Capsule Neural Network for Drowsiness Detection

The proposed CapsNet model for drowsiness detection was used to analyze the data in the ‘ULg Multimodality Drowsiness Database’ (also called DROZY) (Massoz et al., 2016). This dataset was obtained by the Laboratory of Exploitation of Signals and Images (INTELSIG).

The database was collected from 14 completely healthy young subjects who were subjected to three psychomotor vigilance tests (PVT1, 2 and 3) of 10 minutes duration, where the subjects had to monitor a red rectangular box over a black background on a computer screen and to press a button as soon as a yellow figure appeared inside the red rectangle. To ensure the drowsy state of the subjects, they were induced into a prolonged waking state during the tests. Figure 6 shows the schedule of the tests and also the sleep deprivation times used to carry out the experiment.

For each subject and psychomotor vigilance test, the database contains:

DAY 1					DAY 2				
7:00	8:30	10:00	11:00	12:00	20:30	3:30	4:00	12:00	12:30
			PVT1				PVT2		PVT3
Subject free		Subject at the lab.		Subject free + actigraph		Subject at the lab.			
Normal sleep		Sleep deprivation							
					No stimulant				

Figure 6: Summary of data collection schedule Massoz et al. (2016).

- The Karolinska sleepiness scale scores (KSS).
- The stimulus and reaction times of the tests.
- Five EEG channels (Fz, Cz, Pz, C3, and C4) sampled at 512 Hz.
- Two electrooculography channels (EOG) sampled at 512 Hz.
- Electrocardiogram (ECG) sampled at 512 Hz.
- Electromyography (EMG) sampled at 512 Hz.
- Kinect v2 sensor images.
- Kinect v2 sensor videos and face signals.

The DROZY database is perfectly synchronized over time Massoz et al. (2016).

The CapsNet model was able to deal with the spectrogram from EEG with a resolution of 32×32 pixels for a single "Fz channel" and also with 64×32 pixels when the vertical concatenation of channels Fz (at the top) and Pz (at the bottom) were used.

A grid search was performed over all the hyperparameters for a Capsule Neural Network (which is described later in this section) in order to analyze different architectures.

The summary of the proposed models' layers and architecture is described as follows:

1. One convolutional layer with 64 filters and a kernel size of 5×5 with stride 2, which leads to 64 features maps.

- For 32×32 images, each feature map has a size of 14×14 .
 - For 64×32 images, each feature map has a size of 30×14 .
2. A second convolution layer with 128 filters and a kernel size of 9×9 with stride 2 is applied.
 3. The Primary Capsules layer, consisting of 8 capsules with a dimension of 16. Each resulting Primary Capsules layer has a feature map size of 3×3 for input images of 32×32 and 11×3 for the input images of 64×32 .
 4. After the Primary Capsules are formed, each vector is resized using Equation (2), in order to ensure that the length is between 0 and 1.
 5. The prediction of each capsule in the Primary Capsule layer is obtained applying the dynamic routing process 5 times, which is performed using Equations (3), (4), (5) and (6).
 6. The prediction was performed by the dynamic routing process that leads into the Secondary Capsules, which consists of 2 capsules, referred to the base and drowsy states, each one with a dimension of 10. In this step, the length of the instantiation vector of each secondary capsule represents the probability of each state. The desired classification is made considering the highest probability value.
 7. The output of each Secondary Capsule is also fed into a decoder which consists of three fully connected layers:
 - The first with 512 neurons and ReLu activation.
 - The second with 1024 and also ReLu activation
 - The third fully connected layer has a number of neurons equal to the size of the input data (i.e. either 32×32 or 64×32) with Sigmoid activation.
 8. Finally, the squared differences between the output of the decoder and the original input image are calculated, scaled by 0.0005 and added to the margin loss during the training in order to avoid the overfitting of the network.
- All the values used for the hyperparameters were obtained through a grid search. In the first place, the number of feature maps of each convolutional layer was

selected testing from 64 up to 256 features maps. The kernel size of the convolutional layers was selected among five values (3, 5, 7, 9 and 11). For the number of primary capsules and its dimensions, three different options were considered (8, 16, and 32) according to the number of feature maps of the second convolutional layer. Analogously, the dimension of the secondary capsules was tuned by trying out four different values (10, 16, 20 and 24). The number of routing iterations was also tuned considering 5 different options (sequence from 1 up to 5 with a step of 1), which resulted in a value of 5 (in contrast to the 3 routing iterations as used in Sabour et al. (Sabour et al., 2017)). Finally, for the reconstruction error, six options were considered (from 0 to 0.00005, dividing by 10 in each step).

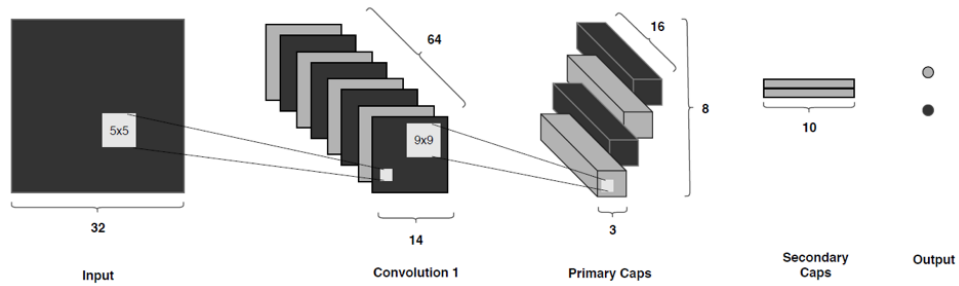


Figure 7: CapsNet architecture for 32x32 spectrograms.

5.2. Experiment 2.- Convolutional Neural Network Model

To assess the effectiveness of the proposed CapsNet model in the drowsiness detection task, its results are compared to the ones obtained from a CNN model. In fact, it is proposed a CNN model with architecture based on Yu-Chia Hung (Hung et al., 2017). The original network in (Hung et al., 2017) was developed to face the same classification problem as here, however using a different (non-public) database and with a different input signal shape. Thus, the architecture developed by Yu-Chia Hung was modified to allow input images with a size of 32×32 , corresponding to the single

Fz channel spectrograms, and images of 64×32 pixels, corresponding to the vertical concatenation of the spectrograms of the Fz and Pz channels.

Indeed, after the input layer, the proposed CNN consists of a 3×3 convolutional layer with 32 features maps, followed by a max-pooling layer with a size of 2×2 or 4×2 depending the case (i.e., 2×2 for 32×32 images and 4×2 for 64×32 images) using a stride of 2 and zero-padding. This structure of convolution-pooling layers is replicated three times, maintaining the size for the pooling layers and varying only the number of features maps for the convolutional layers: 32, 64 and 128 for the first, second and third convolutional layers, respectively. Then, the CNN model has a single fully connected layer with 512 hidden neurons, which is responsible for carrying out the desired drowsiness detection. Figure 8 shows the CNN's architecture for dealing with 32×32 images and can be summarized as:

$$\begin{aligned} \text{Input} = [Z \times 32] - 32C[3 \times 3] - 32P[A \times 2] - 64C[3 \times 3] \\ - 64P[A \times 2] - 128C[3 \times 3] - 128P[A \times 2] - FC[512] - \text{Output}[2] \quad (7) \end{aligned}$$

where C indicates the convolutional layers; P the pooling layers and FC the fully connected layer. The number before each letter indicates the number of filters of each layer; and the number in brackets shows the size of each filter or the number of hidden neurons. Depending on the data set used as input (i.e., 32×32 or 64×32), the letter Z has a value of 32 or 64 and, in the same way has a value of 2 or 4.

Also, to avoid the overfitting of the network, Dropout with keep probability of 0.5 is used in the fully connected layer and $L2$ regularisation with parameter β of 0.001 was applied to the cost function. These parameters, like the size of the kernel of the convolutional layers and the number of hidden neurons in the classification layer, were obtained through a grid search. For the dropout value, we searched among seven options (sequence from 0 to 0.6 with a step of 0.1), and for the β value were explored six options from 0 to 0.0001, dividing by 10 in each step. On the other hand, the size of the kernel of the convolutional layer was picked among three options (3×3 , 5×5 and 7×7), and four options were evaluated for the number of neurons in the classification

Table 2: Summary of performance metrics for the different datasets using CNN and CapsNet. DA represents Data-Augmentation Technique.

Dataset	Model	Accuracy (%)			F1 Score (%)			Sensitivity (%)			Specificity (%)			Precision (%)		
			+/-			+/-			+/-			+/-		+/-		
Fz	CNN	79,46	+/-	4,60	79,55	+/-	4,36	80,80	+/-	3,95	78,07	+/-	5,41	78,30	+/-	4,96
	Caps Net	84,45	+/-	0,62	83,76	+/-	0,65	85,81	+/-	0,97	83,26	+/-	0,91	81,81	+/-	0,81
	Caps Net-DA	89,12	+/-	0,90	87,65	+/-	0,87	89,60	+/-	0,90	88,65	+/-	0,88	87,65	+/-	0,85
Fz-Pz	CNN	75,86	+/-	2,39	76,93	+/-	3,24	79,47	+/-	5,54	71,98	+/-	2,82	74,67	+/-	2,68
	Caps Net	86,74	+/-	1,57	85,97	+/-	1,53	87,57	+/-	4,67	86,53	+/-	4,29	85,20	+/-	3,52
	Caps Net-DA	91,24	+/-	0,95	90,25	+/-	0,85	89,65	+/-	0,90	86,65	+/-	0,91	87,65	+/-	0,87

layers (128, 256, 512 and 1024). Finally, ADAM optimiser was employed, and 500 epochs were used for the model training.

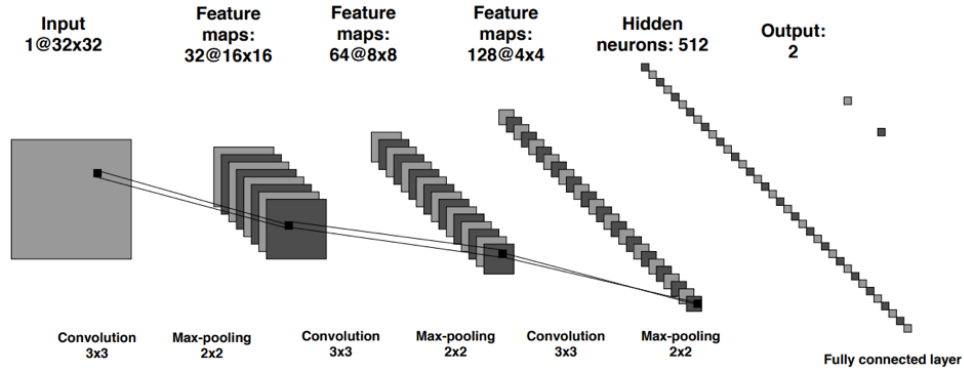


Figure 8: CNN architecture for 32×32 spectrograms.

6. Results and Discussion

6.0.1. CapsNet and CNN models

Table 2 shows the average results with their respective standard deviations for each performance metric in the detection of subjects under drowsiness for both datasets Fz and Fz-Pz, and considering the proposed CapsNet model and the CNN model even with Data-Augmentation.

Figure 9 and Figure 10 outlines the confusion matrices for both the CNN and CapsNet, respectively, for the two datasets: Fz and Fz-Pz. The values presented in Figure 9 and Figure 10 are horizontally normalized by class. Note that the results in Table 2 were obtained from these confusion matrices.

As it can be seen in Table 2, the proposed CapsNet model reaches better average results than CNN for both datasets for all the performance metrics with and without data-augmentation. Indeed, CapsNet reaches 84.45% of accuracy for the Fz dataset and 86.74% for the dataset Fz-Pz dataset, versus the 79.46% and 75.86% reached by the CNN, respectively. Moreover, sensitivity is an important metric in drowsiness detection since it represents the ability of a model to detect subjects who are effectively in a state of drowsiness.

The CapsNet has a sensitivity score of 85.81% for the Fz dataset and 87.57% for the Fz-Pz dataset versus the 80.80% and the 79.47% obtained by the CNN, respectively. These results are also corroborated in Figure 9 and in Figure 10, where the confusion matrices show that the CapsNet is better than CNN in detecting drowsy subjects who are really with drowsiness.

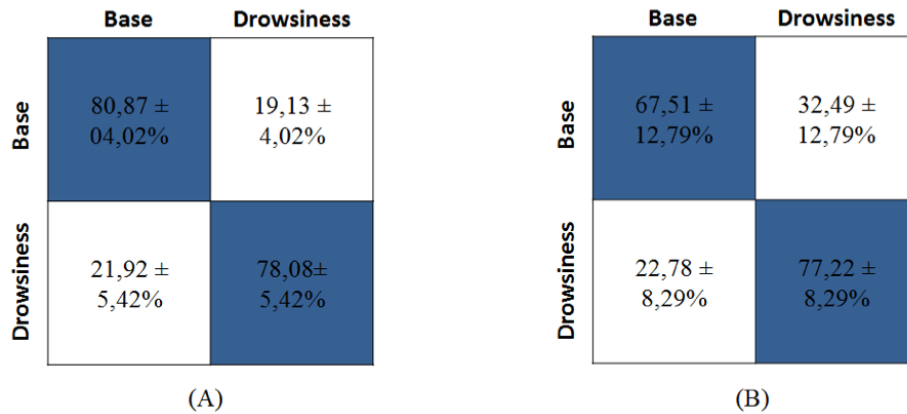


Figure 9: Confusion matrices without Data-augmentation for the CNN models using (A) single Fz channel spectrograms and (B) the vertical concatenation of the Fz-Pz channels.

The proposed CapsNet model also gives smaller standard deviations for all the

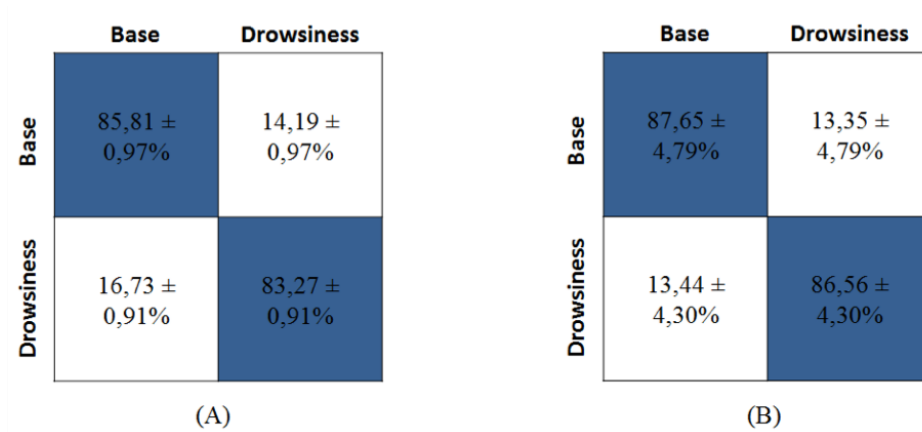


Figure 10: Confusion matrices without Data-augmentation for the CapsNets models using (A) single Fz channel spectrograms and (B) the vertical concatenation of the Fz-Pz channels.

performance metrics. For instance, CapsNet model has a standard deviation of 0.97% for sensitivity, which is the maximum standard deviation value for all the evaluated metrics in the Fz dataset. On the other hand, the standard deviation for the sensitivity in case of the CNN model in the Fz dataset is 3.95%, which is more than four times greater than the one obtained by the CapsNet. These results corroborate the observation that the CapsNet model has a better performance when dealing with smaller datasets, which is an important advantage when working with biomedical signals.

Furthermore, it can be observed that there are differences in the results from each model using the different datasets. Indeed, the CapsNet model gives better average results for each of the evaluated performance metrics when processing the dataset with the joint use of the Fz-Pz channels. However, this increase in the average comes at a cost of an increase in the standard deviation of each one of the metrics. Also, note that the CNN model's performance deteriorates in terms of all metrics in Table 2 when detecting drowsy individuals based on the fusion of Fz and Pz electrodes.

It should be mentioned that the use of only the Pz channel was not considered since in our experiments, its isolated use only reached a 64.78% of accuracy, which would not allow the detection of subjects with drowsiness, which is consistent with previous

research (Jacob et al., 2019). Indeed, the different results for each dataset can be explained by two main facts. Firstly, as demonstrated in (Trejo et al., 2015), the presence of drowsiness in a subject is related to an increase of power in theta waves (tracked by the Fz channel) and a decrease in alpha power (tracked by the Pz channel). Thus, when a subject is under drowsiness, he or she suffers a large phasic increase (event-related) in theta waves, but a tonic decrease (related to life cycle or psychological state) in alpha waves. Moreover, the alpha frequency band has large inter-individual differences associated to age and memory performance (Klimesch, 1999).

Based on these results, one can argue that although the Pz channel provides useful information regarding the state of drowsiness of the subject, this information is related to inherent characteristics of each subject, (as age, gender or mental state). Thus, the model cannot effectively use the signal from the Pz channel to generalise between different subjects, and the drowsiness detection model interprets some characteristics delivered by the Pz channel as noise, leading to a less stable model.

6.0.2. Comparison to shallow models

To have a fair basis of comparison, the SVM and the Random Forest models were submitted to hyperparameter optimisation of the SVM and the Random Forest by means of grid search. As a result, a linear kernel and a penalisation cost of 0.1 were obtained for the SVM. The Random Forest model was trained using 1,024 trees, a max depth of 25 and a min sample leaf of 1. To assess and quantify the importance and quality of automatic features extraction done by the Deep Learning models (CapsNet and CNN) from EEG signals, the shallow Neural Network model in this section was trained using only one hidden layer of 512 neurons.

Table 3 shows the performance of three shallow machine learnings models (Support Vector Machines, Random Forest and a Neural Network) for the same classification task based on the same datasets. For them, the input is the individual pixels of the corresponding spectrograms.

Based on the results reported in Table 3, none of these models reaches an accuracy higher than 80% in the drowsiness detection. In contrast, the proposed CapsNet model delivered an accuracy of 86.74%. Moreover, the shallow models have, on average,

Table 3: Summary of performance metrics for the different datasets using SVM, RF, and NN.

Dataset	Model	Accuracy (%)			F1 Score (%)			Sensitivity (%)			Specificity (%)			Precision (%)		
Fz	SVM	67.28	+/-	3.06	66.13	+/-	3.65	63.85	+/-	4.13	70.84	+/-	6.00	69.94	+/-	6.07
	RF	73.58	+/-	3.39	72.00	+/-	3.66	68.12	+/-	6.42	79.71	+/-	8.81	77.48	+/-	8.62
	NN	69.59	+/-	2.46	68.11	+/-	4.11	65.62	+/-	7.73	72.97	+/-	7.10	71.29	+/-	2.10
Fz-Pz	SVM	71.30	+/-	3.67	72.59	+/-	1.83	72.16	+/-	3.46	69.58	+/-	9.88	73.25	+/-	3.86
	RF	72.50	+/-	4.90	71.00	+/-	5.63	68.28	+/-	7.58	76.68	+/-	2.82	74.11	+/-	3.49
	NN	67.28	+/-	3.06	66.13	+/-	3.65	63.85	+/-	4.13	80.69	+/-	7.31	74.99	+/-	7.26

standard deviations that are significantly greater than both CapsNet and CNN models. Indeed, the higher standard deviation value for each shallow model in the Fz dataset (considering all the evaluated metrics) was 6.07%, 8.81% and 7.73% for the SVM, Random Forest and Neural Network, respectively. If we compare these values with the standard deviation obtained by the CapsNet model, we have between six and nine times greater standard deviation for the shallow models than for the CapsNet model: the shallow models have a higher variability and a diminished capability of generalization.

Based on these results, it can be inferred that the automatic feature extraction made by the convolution layers is essential when working with spectrograms images from EEG signals. In particular, the shallow neural network trained with the same architecture for the hidden layer as in the CNN model presents a significantly variable performance, which corroborates the importance of the use of convolution layers for the feature extraction. In this sense, the CapsNet model takes advantage of the convolutional layer to extract representative features from the EEG spectrograms and also can handle small datasets through the dynamic routing algorithm, delivering a smaller model variability.

Furthermore, the results in Table 3 present a variability of up to 10% between accuracy and precision, which indicates that the shallow models cannot handle the drowsiness detection in a balanced way. That is, despite that the shallow models can reach a specificity of 79.71%, as it is the case of the Random Forest model for the Fz dataset, the same model reaches a sensitivity of only 68.12% for the same dataset, hence, it would be able to correctly classify the subjects without drowsiness, but it would not be able to detect subjects with drowsiness.

Table 4, present a comparison among drowsiness detection models using "ULg Datasets". Based on Table 4, one can observe that the proposed model achieves higher accuracy than all the other models except by the model proposed by Garcia et.al (García-García et al., 2018) which uses video as input data. In this sense, we can divide the models from Table IV in three groups: the ones that need a camera to obtain the input data (image or video), the models that uses biological data as input, and finally the model from by Massoz et. al (Maftukhaturrizqoh et al., 2019), which originally presented the "ULg Multimodality Drowsiness Database" and that uses the time reaction from the psychomotor vigilance tests to detect drowsiness. First, one should note that the model presented by Massoz et. al (Maftukhaturrizqoh et al., 2019) can just be used as a comparison, because the time of reactions is not a data that can be collected continuously in a real car driving situation or in a work environment, so it is not applicable for real-time detection. On the other hand, the model proposed by Maftukhaturrizqoh et.al (Maftukhaturrizqoh et al., 2019) uses electrocardiography (ECG) signals to achieve de detection of drowsiness, using various handcrafted features from the ECG signals, such as the time interval between two consecutive heartbeats. Although this model takes into account the operator privacy (not using any camera device), its accuracy is below the values reached by our proposed model. Finally, from the two models proposed by Garcia et.al (García-García et al., 2018), the one that uses facial images as input reached a lower accuracy than our model, but the one that uses video sequences achieve higher results. However, these two models have two main limitations. In the first place, both models require a video device in front of the subject, which makes these techniques too invasive to the subject's privacy. In second place, an investigation conducted by Ngxande et.al (Ngxande et al., 2019) shows that models that are trained for drowsiness detection with public databases such as the "ULg Multimodality Drowsiness Database" and use image or video sequences as input, do not generalize well when are tested on dark-skinned people due to the bias that the databases can have in terms of ethnical diversity. In this context, in the work conducted by Garcia et.al (García-García et al., 2018), when they tested their model with real-world data, they achieved a much lower accuracy of 68.7% using images as input and a 72.73% of accuracy using video sequences, which corroborates the work presented in Ngxande

et.al (Ngxande et al., 2019). The sixth row of Table 4 shows our best results with and without data-augmentation.

Table 4: Comparison among drowsiness detection models using the “ULg Multimodality Drowsiness Database”. DA represents Data Aumentation.

Author	Metric	Classifier	Accuracy (%)
(Ngxande et al., 2019)	Time Reaction	Support Vector Machine	78.46
(Mafukhaturrizqoh et al., 2019)	ECG Features	Neural Network	81.60
(García-García et al., 2018)	Subject Image	Convolutional Neural Network	85.68
García-García et al. (2018)	Subject Video	Convolutional Neural Network	91.07
Proposed Model	EEG Spectrogram	Capsule Network	86.74 / 91.24 (DA)

Overall, it can be argued that, of all the above deep and shallow models, the CapsNet model is the only one capable of a stable drowsiness detection as it has a standard deviation smaller than 1%. The relevance of this result lies in the amount of data available to train the models (920 samples in total), as it is usually the challenging case when dealing with biomedical data, which in turn represents a severe limitation when developing Deep Learning models.

7. Conclusions

The detection of drowsiness is currently one of the most relevant challenges to guarantee safety and reliability in several industry sectors.

Another challenge involving drowsiness detection is the paucity of biomedical data that imposes severe limitations when developing deep learning models for drowsiness detection. These models require massive amounts of data for the learning and training process.

As a tentative to circumvent this challenge, this work presented a new approach using the Capsule Neural Network model to perform drowsiness detection. Based on the results, with and without data-augmentation presented in Section 4, the proposed CapsNet model is capable of delivering better results than CNN and other shallow machine learning models such as Support Vector Machines, Random Forest and Neural Networks to work with small datasets and transient biological signals such as EEG. This is partially due to the capsules' ability and advantages in working with small amounts of data and because they do not have the positional invariance problems of CNNs as well as the capability of CapsNet to keep the spatial and hierarchical relationships among the extracted features, which results in improved generalization capacity.

Also, it was shown that spectrograms from the frontal (Fz) and parietal (Pz) electrodes could be used as inputs to the drowsiness detection models due to the relationship between the level of drowsiness of a subject and the variations in the amplitude in the range of theta and alpha waves tracked by the frontal (Fz) and parietal (Pz) channels, respectively. In this context, despite the combined use of the frontal (Fz) and parietal (Pz) signals' spectrograms achieved slightly superior results in all the evaluated metrics when compared to the spectrograms obtained from the signals tracked by the frontal (Fz) electrode alone, the use of the single frontal channel provides standard deviations up to four times lower in the evaluated metrics than the results from the fusion of both electrodes, thus suggesting that it represents a more stable and reliable model for drowsiness detection.

On the other hand, since the most challenging step in the development of Deep Learning applications is the training process, which requires high computational resources (characteristics of the used machine for training are described in Section 4), after this step, the already trained model can be easily imported into a portable computer or mobile phone, since the trained model does not require any specific overwhelming requirements to operate, allowing the implementation of a wearable drowsiness identification system.

Therefore, based on the results reported in this study, it can be argued that Capsule Neural Networks are a promising approach for drowsiness detection and are worth further research and development.

8. Future Work

As future work, a new database will be developed in order to study the influence of Occipital electrodes' signals and how this information allows us to improve the drowsiness detection.

References

- (2017). *Niedermeyer's Electroencephalography: Basic Principles, Clinical Applications, and Related Fields (7 ed.)*. Oxford University Press.
- Afshar, P., Mohammadi, A., & Plataniotis, K. N. (2018). Brain tumor type classification via capsule networks. In *2018 25th IEEE International Conference on Image Processing (ICIP)* (pp. 3129–3133). doi:10.1109/ICIP.2018.8451379.
- Akerstedt, T., & Gillberg, M. (1990). Subjective and objective sleepiness in the active individual. *International Journal of Neuroscience*, 52, 29–37.
- ASCH (2007). Antecedentes sobre fatiga en la conduccion de vehiculos. (pp. 16–20). Boletin tecnico. URL: <https://www.achs.cl/portal/Comunidad/Paginas/Campana-Fatiga.aspx>.
- Barua, S., Ahmed, M. U., Ahlstr m, C., & Begum, S. (2019). Automatic driver sleepiness detection using eeg, eog and contextual information. *Expert Systems with Applications*, 115, 121 – 135. URL: <http://www.sciencedirect.com/science/article/pii/S0957417418304792>. doi:<https://doi.org/10.1016/j.eswa.2018.07.054>.
- Boureau, Y.-L., Ponce, J., & LeCun, Y. (2010). A theoretical analysis of feature pooling in visual recognition. In *Proceedings of the 27th International Conference on International Conference on Machine Learning ICML'10* (pp. 111–118). USA: Omnipress. URL: <http://dl.acm.org/citation.cfm?id=3104322.3104338>.
- Breiman, L. (2001). Random forests. *Machine Learning*, 45, 5–32. URL: <https://doi.org/10.1023/A:1010933404324>. doi:10.1023/A:1010933404324.

- Chui, K. T., Tsang, K. F., Chi, H. R., Wu, C. K., & Ling, B. W. (2015). Electrocardiogram based classifier for driver drowsiness detection. In *2015 IEEE 13th International Conference on Industrial Informatics (INDIN)* (pp. 600–603). doi:10.1109/INDIN.2015.7281802.
- Cortes, C., & Vapnik, V. (1995). Support-vector networks. *Machine Learning*, *20*, 273–297. URL: <https://doi.org/10.1023/A:1022627411411>. doi:10.1023/A:1022627411411.
- David Rawlinson, G. K., Abdelrahman Ahmed (2018). Sparse unsupervised capsules generalize better. *ArXiv*, .
- Deng, J., Dong, W., Socher, R., Li, L., Kai Li, & Li Fei-Fei (2009). Imagenet: A large-scale hierarchical image database. In *2009 IEEE Conference on Computer Vision and Pattern Recognition* (pp. 248–255). doi:10.1109/CVPR.2009.5206848.
- García-García, M., Caplier, A., & Rombaut, M. (2018). Sleep deprivation detection for real-time driver monitoring using deep learning. In A. Campilho, F. Karray, & B. ter Haar Romeny (Eds.), *Image Analysis and Recognition* (pp. 435–442). Cham: Springer International Publishing.
- Goodfellow, I., Bengio, Y., & Courville, A. (2016). *Deep Learning*. The MIT Press.
- Hinton, G. E., Sabour, S., & Frosst, N. (2018). Matrix capsules with EM routing. In *International Conference on Learning Representations*.
- Hockey, G., Hockey, R., Gaillard, A., Burov, O., & Division, N. A. T. O. S. A. (2003). *Operator Functional State: The Assessment and Prediction of Human Performance Degradation in Complex Tasks*. NATO science series: Life and behavioural sciences. IOS Press. URL: <https://books.google.cm/books?id=FoDPLDGi-aUC>.
- Homan, R. W. (1988). The 10-20 electrode system and cerebral location. *American Journal of EEG Technology*, *28*, 269–279. URL: <https://doi.org/10.1080/00029238.1988.11080272>. doi:10.1080/00029238.1988.11080272. arXiv:<https://doi.org/10.1080/00029238.1988.11080272>.

- Hung, Y., Wang, Y., Prasad, M., & Lin, C. (2017). Brain dynamic states analysis based on 3d convolutional neural network. In *2017 IEEE International Conference on Systems, Man, and Cybernetics (SMC)* (pp. 222–227). doi:10.1109/SMC.2017.8122606.
- Jacob, C., de Naurois, Bourdin, C., Stratulat, A., Diaz, E., & Vercher, J.-L. (2019). Detection and prediction of driver drowsiness using artificial neural network models. *Accident Analysis and Prevention*, *126*, 95 – 104. URL: <http://www.sciencedirect.com/science/article/pii/S0001457517304347>. doi:<https://doi.org/10.1016/j.aap.2017.11.038>. 10th International Conference on Managing Fatigue: Managing Fatigue to Improve Safety, Wellness, and Effectiveness.
- Jung, A. B. (2018). *imgaug*. <https://github.com/aleju/imgaug>. [Online; accessed 30-Oct-2018].
- Kaida, K., Takahashi, M., Kerstedt, T. A., Nakata, A., Otsuka, Y., Haratani, T., & Fukasawa, K. (2006). Validation of the karolinska sleepiness scale against performance and eeg variables. *Clinical Neurophysiology*, *117*, 1574 – 1581. URL: <http://www.sciencedirect.com/science/article/pii/S1388245706001428>. doi:<https://doi.org/10.1016/j.clinph.2006.03.011>.
- Klimesch, W. (1999). Eeg alpha and theta oscillations reflect cognitive and memory performance: a review and analysis. *Brain Research Reviews*, *29*, 169 – 195. URL: <http://www.sciencedirect.com/science/article/pii/S0165017398000563>. doi:[https://doi.org/10.1016/S0165-0173\(98\)00056-3](https://doi.org/10.1016/S0165-0173(98)00056-3).
- LaLonde, R., & Bagci, U. (2018). Capsules for object segmentation. *CoRR*, *abs/1804.04241*.
- LeCun, Y., Bengio, Y., & Hinton, G. (2015). Deep Learning. *Nature*, *521*, 436–444. URL: <https://www.nature.com/articles/nature14539>. doi:10.1038/nature14539.

- LeCun, Y., & Cortes, C. (2010). MNIST handwritten digit database, . URL: <http://yann.lecun.com/exdb/mnist/>.
- Lee, H., Pham, P., Largman, Y., & Ng, A. Y. (2009). Unsupervised feature learning for audio classification using convolutional deep belief networks. In Y. Bengio, D. Schuurmans, J. D. Lafferty, C. K. I. Williams, & A. Culotta (Eds.), *Advances in Neural Information Processing Systems 22* (pp. 1096–1104). Curran Associates, Inc.
- Lees, W. M., Wunderlich, A., Jeavons, P., Hale, P. D., & Souryal, M. R. (2019). Deep learning classification of 3.5-ghz band spectrograms with applications to spectrum sensing. *IEEE Transactions on Cognitive Communications and Networking*, 5, 224–236.
- Maftukhaturrizqoh, O., Nuryani, N., & Darmanto, D. (2019). Drowsiness detection using radial basis function network with electrocardiographic RR interval statistical feature. *Journal of Physics: Conference Series*, 1153, 012049.
- Marek, T., Noworol, C., & Karwowski, W. (1988). Mental fatigue at work and pain perception. *Work & Stress*, 2, 133–137. doi:10.1080/02678378808259157.
- Massoz, Q., Langohr, T., François, C., & Verly, J. G. (2016). The ulg multimodality drowsiness database (called drozy) and examples of use. In *2016 IEEE Winter Conference on Applications of Computer Vision (WACV)* (pp. 1–7). doi:10.1109/WACV.2016.7477715.
- Ngxande, M., Tapamo, J., & Burke, M. (2019). Detecting inter-sectional accuracy differences in driver drowsiness detection algorithms. *CoRR*, abs/1904.12631. URL: <http://arxiv.org/abs/1904.12631>.
- Pan, Q., Li, X., & Fang, L. (2020). Data augmentation for deep learning-based ecg analysis. In C. Liu, & J. Li (Eds.), *Feature Engineering and Computational Intelligence in ECG Monitoring* (pp. 91–111). Singapore: Springer Singapore.
- Park, D. S., Chan, W., Zhang, Y., Chiu, C.-C., Zoph, B., Cubuk, E. D., & Le, Q. V. (2019). SpecAugment: A Simple Data Augmentation Method

- for Automatic Speech Recognition. In *Proc. Interspeech 2019* (pp. 2613–2617). URL: <http://dx.doi.org/10.21437/Interspeech.2019-2680>. doi:10.21437/Interspeech.2019-2680.
- Ramzan, M., Khan, H. U., Awan, S. M., Ismail, A., Ilyas, M., & Mahmood, A. (2019). A survey on state-of-the-art drowsiness detection techniques. *IEEE Access*, 7, 61904–61919. doi:10.1109/ACCESS.2019.2914373.
- Sabour, S., Frosst, N., & Hinton, G. E. (2017). Dynamic routing between capsules. In I. Guyon, U. V. Luxburg, S. Bengio, H. Wallach, R. Fergus, S. Vishwanathan, & R. Garnett (Eds.), *Advances in Neural Information Processing Systems 30* (pp. 3856–3866). Curran Associates, Inc.
- Schmidhuber, J. (2015). Deep learning in neural networks: An overview. *Neural Networks*, 61, 85 – 117. URL: <http://www.sciencedirect.com/science/article/pii/S0893608014002135>. doi:<https://doi.org/10.1016/j.neunet.2014.09.003>.
- Sokolova, M., & Lapalme, G. (2009). A systematic analysis of performance measures for classification tasks. *Inf. Process. Manage.*, 45, 427–437. URL: <http://dx.doi.org/10.1016/j.ipm.2009.03.002>. doi:10.1016/j.ipm.2009.03.002.
- Spampinato, C., Palazzo, S., Kavasidis, I., Giordano, D., Souly, N., & Shah, M. (2017). Deep learning human mind for automated visual classification. In *2017 IEEE Conference on Computer Vision and Pattern Recognition (CVPR)* (pp. 4503–4511). doi:10.1109/CVPR.2017.479.
- Trejo, L. J., Kubitz, K., Rosipal, R., Kochavi, R. L., & Montgomery, L. D. (2015). "eeg based estimation and classification of mental fatigue". *Psychology*, 05.
- Upadhyay, Y., & Schrater, P. (2018). Generative adversarial network architectures for image synthesis using capsule networks. *CoRR*, *abs/1806.03796*.

- Verstraete, D., Ferrada, A., Droguett, E. L., Meruane, V., & Modarres, M. (2017). Deep learning enabled fault diagnosis using time-frequency image analysis of rolling element bearings.
- Xi, E., Bing, S., & Jin, Y. (2017). Capsule network performance on complex data. (p. 1–7). volume 10707.
- Yeo, M. V., Li, X., Shen, K., & Wilder-Smith, E. P. (2009). Can svm be used for automatic eeg detection of drowsiness during car driving? *Safety Science*, *47*, 115 – 124.
- Yuan L., C. J. (2018). Patients eeg data analysis via spectrogram image with a convolution neural network. *Intelligent Decision Technologies. IDT 2017. Smart Innovation, Systems and Technologies*, *72*.
- Zheng, W., Liu, W., Lu, Y., Lu, B., & Cichocki, A. (2019). Emotionmeter: A multi-modal framework for recognizing human emotions. *IEEE Transactions on Cybernetics*, *49*, 1110–1122. doi:10.1109/TCYB.2018.2797176.